Experimental Neurology 283 (2016) 85–96

Contents lists available at ScienceDirect

Experimental Neurology

journal homepage: www.elsevier.com/locate/yexnr

Regulation of astrocyte glutamate transporter-1 (GLT1) and aquaporin-4 (AQP4) expression in a model of epilepsy

Jacqueline A. Hubbard [a], Jenny I. Szu [b], Jennifer M. Yonan [b], Devin K. Binder [b,c,d,*]

[a] Department of Biochemistry and Molecular Biology, University of California, Riverside, USA
[b] Neuroscience Graduate Program, University of California, Riverside, USA
[c] Center for Glial-Neuronal Interactions, University of California, Riverside, USA
[d] Division of Biomedical Sciences, School of Medicine, University of California, Riverside

ARTICLE INFO

Article history:
Received 23 November 2015
Received in revised form 23 April 2016
Accepted 1 May 2016
Available online 4 May 2016

Keywords:
Glutamate transporter-1
GLT1
EAAT2
Aquaporin
AQP4
GFAP
Astrocyte
Seizure
Kainic acid
Epilepsy

ABSTRACT

Astrocytes regulate extracellular glutamate and water homeostasis through the astrocyte-specific membrane proteins glutamate transporter-1 (GLT1) and aquaporin-4 (AQP4), respectively. The role of astrocytes and the regulation of GLT1 and AQP4 in epilepsy are not fully understood. In this study, we investigated the expression of GLT1 and AQP4 in the intrahippocampal kainic acid (IHKA) model of temporal lobe epilepsy (TLE). We used real-time polymerase chain reaction (RT-PCR), Western blot, and immunohistochemical analysis at 1, 4, 7, and 30 days after kainic acid-induced status epilepticus (SE) to determine hippocampal glial fibrillary acidic protein (GFAP, a marker for reactive astrocytes), GLT1, and AQP4 expression changes during the development of epilepsy (epileptogenesis). Following IHKA, all mice had SE and progressive increases in GFAP immunoreactivity and GFAP protein expression out to 30 days post-SE. A significant initial increase in dorsal hippocampal GLT1 immunoreactivity and protein levels were observed 1 day post SE and followed by a marked downregulation at 4 and 7 days post SE with a return to near control levels by 30 days post SE. AQP4 dorsal hippocampal protein expression was significantly downregulated at 1 day post SE and was followed by a gradual return to baseline levels with a significant increase in ipsilateral protein levels by 30 days post SE. Transient increases in GFAP and AQP4 mRNA were also observed. Our findings suggest that specific molecular changes in astrocyte glutamate transporters and water channels occur during epileptogenesis in this model, and suggest the novel therapeutic strategy of restoring glutamate and water homeostasis.

1. Introduction

Epilepsy is a group of disorders characterized by the unpredictable occurrence of seizures. It is a major public health concern and is estimated to afflict one in 26 people in their lifetime (Hesdorffer et al., 2011). Temporal lobe epilepsy (TLE), the most common form of epilepsy, affects over 40 million people worldwide alone (de Lanerolle et al., 2012). Approximately 30% of patients taking antiepileptic drugs (AEDs), however, do not become seizure-free with existing medications. Current AEDs primarily target neurons and often cause severe cognitive, developmental, and behavioral side effects. Therefore, new drugs based on non-neuronal targets are an appealing alternative approach with potentially fewer deleterious effects. Although it has been well established that increased neuronal excitability is a major contributor to epilepsy, increasing evidence suggests that changes in astrocytes contribute to the development of epilepsy (Hubbard et al., 2013).

Astrocytes, a critical component of the tripartite synapse (Araque et al., 1999), participate in ionic homeostasis, energy metabolism (Ransom and Ransom, 2012), the formation of synaptic networks (Ransom et al., 2003), and the modulation of synaptic transmission (Halassa and Haydon, 2010; Murphy-Royal et al., 2015; Volterra and Meldolesi, 2005). Striking changes in astrocytic shape and function are observed in "reactive" cells, often measured by levels of the intermediate filament glial fibrillary acidic protein (GFAP). Based on not only morphological alterations but also functional changes in expression of channels and receptors, reactive astrocytes may contribute to increased neuronal excitability and the development of epilepsy (Binder and Steinhäuser, 2006; Hubbard et al., 2013).

Extracellular glutamate levels determine the extent of neuronal excitability; therefore it is crucial to maintain low glutamate levels in the extracellular space (ECS). Glutamate transporters are responsible

Abbreviations: Antiepileptic drugs, (AEDs); aquaporin-4, (AQP4); central nervous system, (CNS); 4′,6-diamidino-2-phenylindole, (DAPI); electroencephalogram, (EEG); extracellular space, (ECS); glial fibrillary acidic protein, (GFAP); glutamate transporter-1, (GLT1); granule cell layer, (GCL); hippocampal sclerosis, (HS); kilodalton, (KDa); real-time polymerase chain reaction, (RT-PCR); status epilepticus, (SE); stratum lacunosum moleculare, (SLM).

* Correspondence to: Devin K. Binder, Division of Biomedical Sciences, University of California, Riverside, 1247 Webber Hall, Riverside, CA 92521, USA.
E-mail address: dbinder@ucr.edu (D.K. Binder).

http://dx.doi.org/10.1016/j.expneurol.2016.05.003
0014-4886/

for removing glutamate from the ECS. The most prominently expressed glutamate transporter in the mammalian forebrain is glutamate transporter-1 (GLT1) (Danbolt, 2001), found almost exclusively on astrocytes. Deletion (Tanaka et al., 1997) or antisense oligonucleotide-mediated inhibition of synthesis (Rothstein et al., 1996) of GLT1 in rodents revealed that it is the major contributor to glutamate uptake from the ECS. GLT1-mediated glutamate removal from the tripartite synapse is conducted in an activity-regulated manner, thereby shaping synaptic transmission (Murphy-Royal et al., 2015). Furthermore, homozygous mice deficient in GLT1 develop lethal spontaneous seizures (Tanaka et al., 1997). Overexpression of GLT1, on the other hand, attenuated epileptogenesis and reduced seizure frequency in transgenic mice (Kong et al., 2012). It is widely accepted that delayed glutamate clearance from the ECS is implicated in seizures (Campbell and Hablitz, 2004; During and Spencer, 1993; Glass and Dragunow, 1995; Hubbard et al., 2013; Tanaka et al., 1997), but whether changes in GLT1 expression or function underlie the development of epilepsy is unknown.

The aquaporins (AQPs) are a family of small, hydrophobic membrane water channels that facilitate water transport in response to osmotic gradients (Agre et al., 2002; Amiry-Moghaddam and Ottersen, 2003; Binder et al., 2012; Verkman, 2005). Aquaporin-4 (AQP4) is the main water channel in the brain and spinal cord and is expressed by glial cells, especially at specialized membrane domains including astroglial endfeet in contact with blood vessels and astrocyte membranes that ensheathe glutamatergic synapses (Nagelhus et al., 2004; Nielsen et al., 1997; Rash et al., 1998). The creation of AQP4 knockout mice in 1997 (Ma et al., 1997) helped elucidate the various functions of AQP4 in the brain. It is now known that AQP4 plays a role in potassium buffering (Binder et al., 2006), modulation of extracellular space diffusion (Binder et al., 2004), and even in synaptic plasticity and memory (Skucas et al., 2011; Szu and Binder, 2016). Mice deficient in AQP4 have increased seizure duration (Binder et al., 2006) and decreased AQP4 immunoreactivity during the early epileptogenic phase in mouse models of epilepsy (Alvestad et al., 2013; Lee et al., 2012b). AQP4 has been implicated in epilepsy (Binder et al., 2012; Binder et al., 2006; Eid et al., 2005; Lee et al., 2012a; Lee et al., 2012b), but the expression and regulation of AQP4 during epileptogenesis has not been fully characterized.

In this study, we used the well-established intrahippocampal kainic acid (IHKA) mouse model of temporal lobe epilepsy (Arabadzisz et al., 2005; Bouilleret et al., 1999; Riban et al., 2002) to fully examine GFAP, GLT1 and AQP4 regulation during epileptogenesis. We used real-time polymerase chain reaction (RT-PCR), Western blot, and immunohistochemical analysis at 1, 4, 7, and 30 days after IHKA-induced status epilepticus (SE) to determine hippocampal GFAP, GLT1, and AQP4 expression changes during the development of epilepsy. We found a significant initial increase in dorsal hippocampal GLT1 immunoreactivity and protein levels 1 day post SE and a significant downregulation by 7 days post SE. AQP4 dorsal hippocampal protein levels were downregulated at early time points after SE and were upregulated ipsilaterally at 30 days post SE. These results indicate significant downregulation of these critical glial transporters (GLT1 and AQP4) during the early epileptogenic period in this model.

2. Methods

2.1. Animals

All experiments were conducted in accordance with National Institutes of Health guidelines and were approved by the University of California, Riverside Institutional Animal Care and Use Committee (IACUC). Animals were housed under a 12 h light/12 h dark cycle with food and water provided *ad libitum*. 7 to 8-week-old CD1 male mice from Charles River were used for these experiments.

2.2. Surgery

We used intrahippocampal kainic acid (IHKA) injections to induce epileptogenesis (Arabadzisz et al., 2005; Bouilleret et al., 1999; Riban et al., 2002). Briefly, mice were anesthetized with an intraperitoneal (i.p.) injection of a mixture of 80 mg/kg ketamine and 10 mg/kg xylazine and mounted in a stereotaxic frame. An incision was made to expose the skull and bregma was located. Using stereotaxic coordinates of the hippocampus (Paxinos and Franklin, 2001), a 0.6 mm burr hole was made 1.8 mm posterior and 1.6 mm lateral from bregma with a high-speed drill (Drummond Scientific). Mice were injected with either 74 nL of a 20 mM solution of kainic acid or an equal volume of 0.9% saline over a period of 4 min using a microinjector (Nanoject, Drummond Scientific) into the right dorsal hippocampus (dorsoventral coordinate 1.9 mm).

2.3. Kainic acid status epilepticus

After kainic acid injections, all mice experienced status epilepticus (SE), defined by Racine scale stage 3–5 seizures (Racine, 1972) continuously for a period of 3 or more hours. In preliminary studies, we verified the presence of epileptiform activity in 100% of animals after IHKA injections by video-electroencephalogram (EEG) monitoring (Lee et al., 2012b) (Supplemental Fig. S1 in the online version at http://dx.doi.org/10.1016/j.expneurol.2016.05.003.). Within 30 min of IHKA injections, mice experienced SE for several hours, which spontaneously subsided. In this model, mice exhibit spontaneous recurrent seizures in both hippocampi (Supplemental Fig. S1 in the online version at http://dx.doi.org/10.1016/j.expneurol.2016.05.003.). Previous studies in the IHKA model (Arabadzisz et al., 2005; Bouilleret et al., 1999; Riban et al., 2002) demonstrated that the model reproduced morphological characteristics of mesial temporal sclerosis, including neuronal loss, gliosis, mossy fiber sprouting, and dentate granule cell dispersion. We have previously confirmed the pattern of neuronal loss in CA1 and progressive dentate granule cell dispersion as well as performed chronic video-EEG recording in this model (Lee et al., 2012b) (Supplemental Fig. S1 in the online version at http://dx.doi.org/10.1016/j.expneurol.2016.05.003.).

For the current studies, we wished to avoid electrode damage to the brain and therefore proceeded without the use of EEG implantation. Instead, we monitored animals for behavioral seizures. All animals experienced continuous (3 or more hours) Racine stage 3–5 seizures (Racine, 1972), characterized by forelimb and hindlimb clonus, rearing, and falling. Animals that died due to SE were excluded from the study. Otherwise, at each time point $n = 5$ animals were euthanized with fatal plus (Western Medical Supply), perfused, and processed for each experiment, unless otherwise specified.

2.4. Immunohistochemistry

Mice were perfused transcardially with ice-cold phosphate buffered saline (PBS), pH 7.4, followed by 4% paraformaldehyde, pH 7.4. Brains were quickly removed and postfixed in 4% paraformaldehyde overnight at 4 °C followed by two days of cryoprotection in 30% sucrose in PBS at 4 °C. Brains were then cut into 50 μm coronal sections using a cryostat (Leica CM 1950, Leica Microsytems, Bannockburn, IL) and stored in PBS at 4 °C. All slices were processed simultaneously. Endogenous peroxidase activity was quenched by incubating slices in 3% H_2O_2 for 1 h at room temperature. This was followed by a 1 h blocking step with 5% normal goat serum in 0.1 M PBS. Slices were then incubated with primary antibody to GLT1 (1:3000, AbCam AB41621) and GFAP (1:200, Millipore MAB360) in 0.3% Triton X-100 overnight at 4 °C. After washing slices with PBS, sections were incubated with species-specific secondary antibody conjugated with Alexa 488 or 594 and a tyramide signaling amplification (TSA) kit (Molecular Probes/Invitrogen) for visualization. Slices were mounted in Vectorshield with DAPI (Vector Laboratories)

and 10× images were taken using a fluorescence microscope (Leica DFC345 FX). Confocal 40× images were taken on the Leica SP5 inverted microscope.

Quantification was performed using the Leica Application Suite (LAS) X Lite software. Fluorescent images of the hippocampus were captured at 10× magnification under identical settings. A box delineating the region of interest (ROI) was drawn on the DAPI channel either around all layers of the hippocampus or at the center of each layer of the hippocampus: stratum (S.) oriens, S. pyramidale, S. radiatum, S. lacunosum moleculare (SLM), molecular layer, granule cell layer (GCL), and hilus (Supplemental Fig. S2B in the online version at http://dx.doi.org/10.1016/j.expneurol.2016.05.003.). In the CA3 region of the hippocampus, ROIs around the S. lucidum, S. pyramidale, and S. oriens were drawn (Supplemental Fig. S2B in the online version at http://dx.doi.org/10.1016/j.expneurol.2016.05.003.). The mean pixel (gray) value within each ROI was obtained for analysis. For each time point, 4 slices from each animal ($n = 5$) were used.

2.5. Western blot analysis

Dorsal hippocampus was microdissected from the mouse brain at 1, 4, 7, and 30 days post intrahippocampal kainic acid (IHKA) or saline injection ($n = 7$ for 7 days post SE; $n = 5$ for saline control and all other time points). Harvested tissue was homogenized using the Bullet Blender bead homogenizer (Next Advance) in radioimmunoprecipitation assay (RIPA) buffer (150 mM NaCl, 1% NP-40, 0.5 sodium deoxycholate, 0.1% SDS, 50 mM Tris pH 7.5) containing complete protease inhibitors (Roche). Protein concentrations were assayed and protein was resolved by SDS-PAGE, 10% polyacrylamide, and transferred to a nitrocellulose membrane. The membranes were then probed for either AQP4 (1:1000, Millipore ABN411) or GLT1 (1:5000 of a C-terminal polyclonal antibody (Rothstein et al., 1994)) and β-actin (1:10,000, Sigma A1978) as an internal control. Whole hippocampal tissue was microdissected, processed, and probed for GFAP (1:5000, Millipore AB5804), AQP4 (1:1000, Millipore ABN411), or GLT1 (1:10,000, AbCam AB41621; also confirmed with 1:5000 of the C-terminal polyclonal antibody (Rothstein et al., 1994)) while again using β-actin (1:10,000, Sigma A1978) as an internal control. Bands were visualized and quantified using the Li-COR Odyssey Fc Western Imaging System and protein levels of AQP4, GLT1 and GFAP were normalized to internal β-actin levels. The upper (tetrameric) band for AQP4 is shown, was determined to be specific (Supplemental Fig. S3 in the online version at http://dx.doi.org/10.1016/j.expneurol.2016.05.003.), and therefore was used for quantification. For GLT1, both the lower and upper bands are shown but only quantification of the lower band was included for simplicity. Similar results, however, were observed when quantifying the upper band.

2.6. Real-time polymerase chain reaction (RT-PCR) analysis

Whole or dorsal hippocampus was microdissected from the mouse brain at 1, 4, 7, and 30 days post intrahippocampal kainic acid (IHKA) or saline injection. Harvested tissue was homogenized using the Bullet Blender bead homogenizer (Next Advance). RNA was isolated using the Direct-Zol RNA mini prep kit (Zymo Research) and quantified using a nanodrop (Thermo Scientific NanoDrop 2000c Spectrophotometer). Both cDNA synthesis and RT-PCR were performed using the Bioline SensiFAST SYBR NO-ROX Kit and the CFX-96 detection system (Bio-Rad). Primers for AQP4, GLT1, GFAP and 18s RNA (Table 1) were purchased from Integrated DNA Technologies. The reaction conditions were as follows: 1 cycle for 10 min at 45 °C, 1 cycle for 2 min at 95 °C, 40 cycles for 5 s at 95 °C, and 1 cycle for 20 s at 60 °C. Results were quantified using the differential CT method representing the fold change in target gene expression. Both a no template control (NTC) and a no reverse transcriptase (NRT) control were included in each assay to detect any contamination or non-specific replication.

Table 1
Primers used for RT-PCR experiments. All primers are listed in the 5′ → 3′ direction.

Target gene	Forward primer sequence	Reverse primer sequence
AQP4	CTGGAGCCAGCATGAATCCAG	TTCTTCTCTTCTCCACGGTCA
GLT1	CTGGTGCAAGCCTGTTTCC	GCCTGTTCACCCATCTTCC
GFAP	ATCGAGATCGCCACCTACAG	CTTCTTTGGTGCTTTTGCCCC
18s RNA	CTCAACACGGGAAACCTCAC	CGCTCCACCAACTAAGAACG

2.7. Statistical analysis

Statistical analysis was performed using a one-way ANOVA with *post-hoc* Bonferroni multiple comparisons test. All error bars are presented as the mean ± standard error of the mean (SEM). A comparison to saline control was denoted statistically significance by a p-value <0.05, <0.01 or <0.001 and denoted with *, **, or ***, respectively. Any statistically significant differences between other time points were not indicated for the purpose of clarity.

3. Results

3.1. Increased GFAP expression

Hippocampal GFAP and DAPI immunoreactivity were imaged after saline injections (control) and at 1, 4, 7, and 30 days post kainic acid-induced status epilepticus (SE). Analysis of GFAP immunoreactivity revealed a progressive increase in GFAP in the hippocampus ipsilateral to kainic acid injection (Fig. 1). GFAP immunoreactivity was markedly elevated at 4, 7, and 30 days post kainic acid-induced SE compared to the saline control in every layer of the hippocampus except in the stratum (S.) radiatum and stratum lacunosum moleculare (SLM) at 4 days post SE. The formation of a sclerotic hippocampus, as observed here, is a hallmark of temporal lobe epilepsy (TLE). At 1 day post SE, no difference from the saline control was observed. A similar progressive increase in GFAP immunoreactivity was observed in the CA3 region of the ipsilateral hippocampus (Supplemental Fig. S4 in the online version at http://dx.doi.org/10.1016/j.expneurol.2016.05.003.). Higher magnification images of GFAP immunoreactivity in the ipsilateral hippocampus can be seen in Supplemental Fig. S5 in the online version at http://dx.doi.org/10.1016/j.expneurol.2016.05.003..

We next used Western blot and RT-PCR to investigate changes in GFAP hippocampal protein and mRNA levels, respectively (Fig. 2). We found a progressive increase in GFAP protein levels in both the ipsilateral (Fig. 2A–B) and contralateral (Fig. 2D–E) hippocampi. Specifically, no changes in GFAP protein expression were observed 1 day post SE, but a trend towards increased protein was observed 4 days post SE with a significant and persistent increase at 7 and 30 days post SE. GFAP mRNA, on the other hand, showed a significant increase in expression at 1 and 4 days post SE in the ipsilateral hippocampus (Fig. 2C) but only an increase at 1 day post SE in the contralateral hippocampus (Fig. 2F). Taken together, these results suggest that both GFAP mRNA and protein are significantly increased during epileptogenesis in the IHKA model.

3.2. Alterations in glutamate transporter-1 (GLT1) expression

GLT1 and DAPI immunoreactivity in the hippocampus were imaged after saline injections (control) and at 1, 4, 7, and 30 days post kainic acid-induced status epilepticus (SE) (Figs. 3–4). Marked changes in GLT1 immunoreactivity were observed in the ipsilateral hippocampus after IHKA injections (Fig. 3). An initial increase in GLT1 immunoreactivity was observed at 1 day post SE, which subsided by 4 days post SE, was followed by a significant downregulation at 7 days post SE, and returned to near baseline levels by 30 days post SE. More specifically, a significant increase in GLT1 immunoreactivity was observed in all layers of the hippocampus at 1 day post SE (Fig. 3B). By 4 days post SE, GLT1 immunoreactivity was persistently decreased in the primarily astrocytic layers (S.

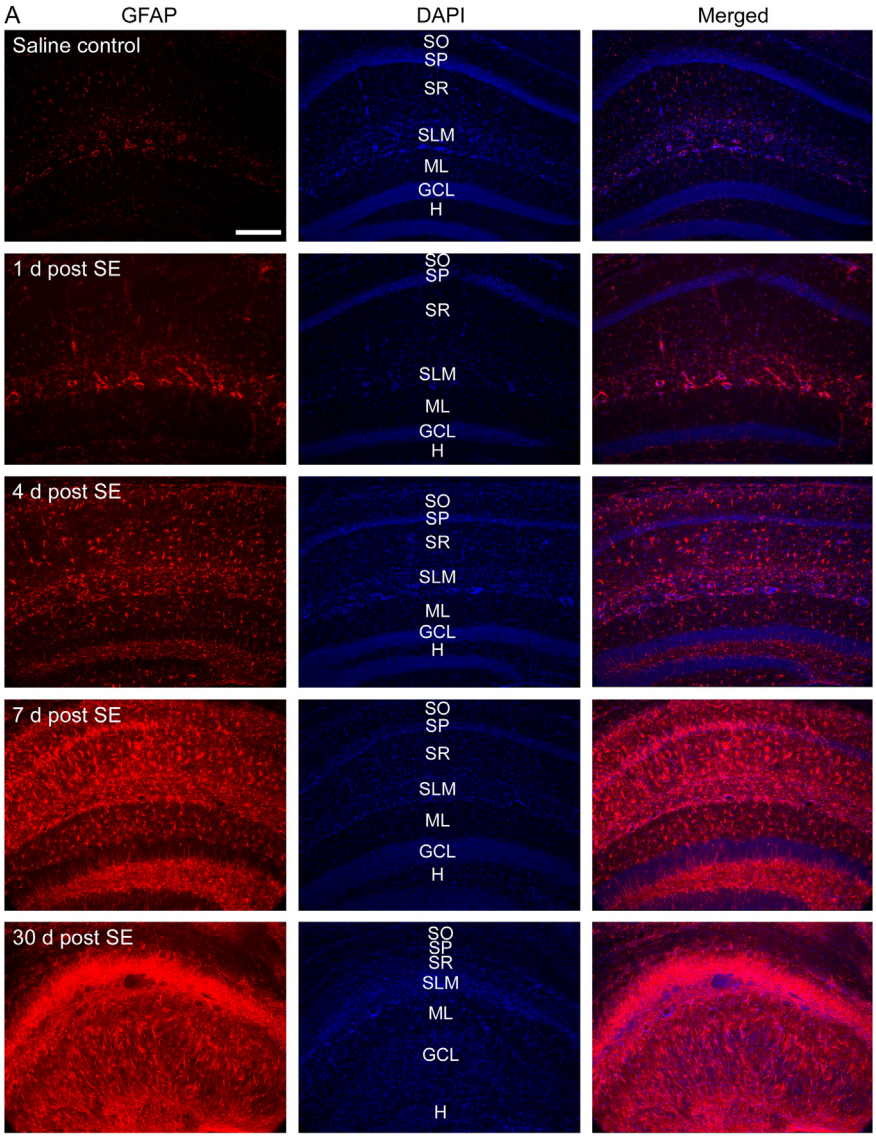

Fig. 1. Glial fibrillary acidic protein (GFAP) immunoreactivity in the ipsilateral hippocampus after kainic acid-induced status epilepticus (SE). A. 10× images of GFAP (red), DAPI (blue), and merged immunoreactivity of the ipsilateral hippocampus after saline injections (Saline control) and 1, 4, 7, and 30 days (d) post SE. B. Quantification of GFAP immunoreactivity in the various layers of the hippocampus. ** indicates $p < 0.01$ and *** indicates $p < 0.001$ when compared to saline control. Scale bar = 200 μm. SO = stratum oriens; SP = stratum pyramidale; SR = stratum radiatum; SLM = stratum lacunosum moleculare; ML = molecular layer; GCL = granule cell layer; H = hilus.

radiatum, SLM, molecular layer) for the remainder of the time course study. In the hilus, however, GLT1 immunoreactivity was downregulated at 4 and 7 days post SE, but returned to baseline levels by 30 days post SE. Similar results were seen in the CA3 region of the ipsilateral hippocampus (Supplemental Fig. S6 in the online version at http://dx.doi.org/10.1016/j.expneurol.2016.05.003.). The neuronal layers, S. pyramidale and granule cell layer (GCL), did not show any downregulation of GLT1 immunoreactivity. In fact, GLT1 levels were elevated at 4 days post SE in the S. pyramidale layer and returned to saline control levels by 7 days post SE. Although GLT1 immunoreactivity was no different from the saline control at 4 and 7 days post SE in the GCL, immunoreactivity was elevated at 30 days post SE. This is likely due to reactive astrocytic processes protruding into the dispersed GCL in the sclerotic hippocampus at this time point (Fig. 1). Higher magnification images of GLT1 and GFAP immunoreactivity in the ipsilateral hippocampus can be seen in Supplemental Fig. S5 in the online version at http://dx.doi.org/10.1016/j.expneurol.2016.05.003.. At 1 and 30 days post SE, GLT1 and GFAP are highly colocalized. Notably, at 4 and 7 days post SE, many GLT1-negative/GFAP-positive astrocytes are seen.

Similar changes in GLT1 immunoreactivity were observed in the contralateral hippocampus (Fig. 4). Throughout the hippocampal layers, GLT1 was downregulated at 4 and 7 days post SE with the exception of the S. oriens at 4 days post SE (Fig. 4B). A significant increase in GLT1 immunoreactivity 1 day post SE was only observed in the SLM and hilus of the contralateral hippocampus. A persistent downregulation of GLT1 immunoreactivity out to 30 days post SE was only detected in the SLM. In the CA3 region of the hippocampus, GLT1 immunoreactivity was downregulated at 4 and 7 days post SE in all layers quantified (Supplemental Fig. S7 in the online version at http://dx.doi.org/10.1016/j.expneurol.2016.05.003.). Thus, downregulation of GLT1 immunoreactivity was observed in *both* ipsilateral and contralateral hippocampi at 4 and 7 days. Higher magnification images of GLT1 immunoreactivity in the contralateral hippocampus can be seen in Supplemental Fig. S8 in the online version at http://dx.doi.org/10.1016/j.expneurol.2016.05.003.. GLT1 and GFAP were highly colocalized in the saline control and 1 day post SE. At 4 and 7 days post SE, many GLT-negative/GFAP-positive astrocytes are seen.

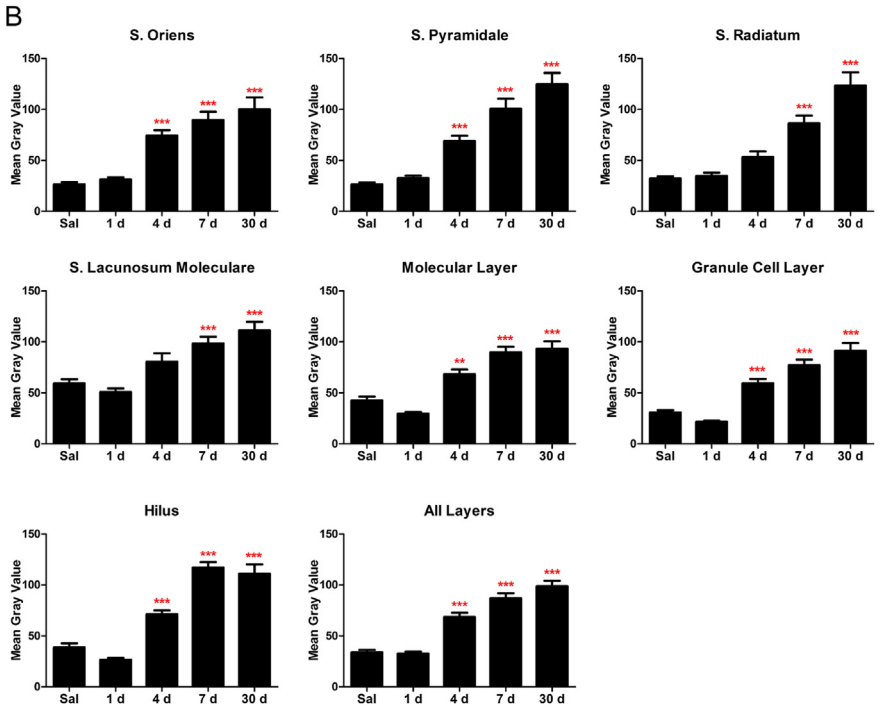

Fig. 1 (*continued*).

Western blot analysis revealed a significant increase in dorsal hippocampal GLT1 protein levels at 1 day post SE followed by a significant downregulation of GLT1 protein levels by 7 days post SE in the ipsilateral hippocampus compared to the saline control (Fig. 5A–B). In the contralateral dorsal hippocampus, significant downregulation of GLT1 protein was found at 4 and 7 days post SE (Fig. 5D–E). These results were consistent with the immunohistochemical findings (Figs. 3–4) both in direction and time course. Quantitative RT-PCR analysis of GLT1 mRNA revealed no changes in GLT1 mRNA levels in either the ipsilateral (Fig. 5C) or contralateral (Fig. 5F) dorsal hippocampus with the exception of an increase in GLT1 mRNA in the ipsilateral hippocampus 7 days post SE. Overall, these results indicate a strong regulation of GLT1 dorsal hippocampal protein levels with an increase at 1 day and significant decreases at 4 and 7 days post SE in this model, with little accompanying change in GLT1 mRNA levels. Separate analysis of whole hippocampal GLT1 protein and mRNA levels revealed no change in protein levels but small decrease in GLT1 mRNA in the ipsilateral hippocampus 1 day post SE and an increase in GLT1 mRNA in the contralateral hippocampus 7 days post SE (Supplemental Fig. S9 in the online version at http://dx.doi.org/10.1016/j.expneurol.2016.05.003.).

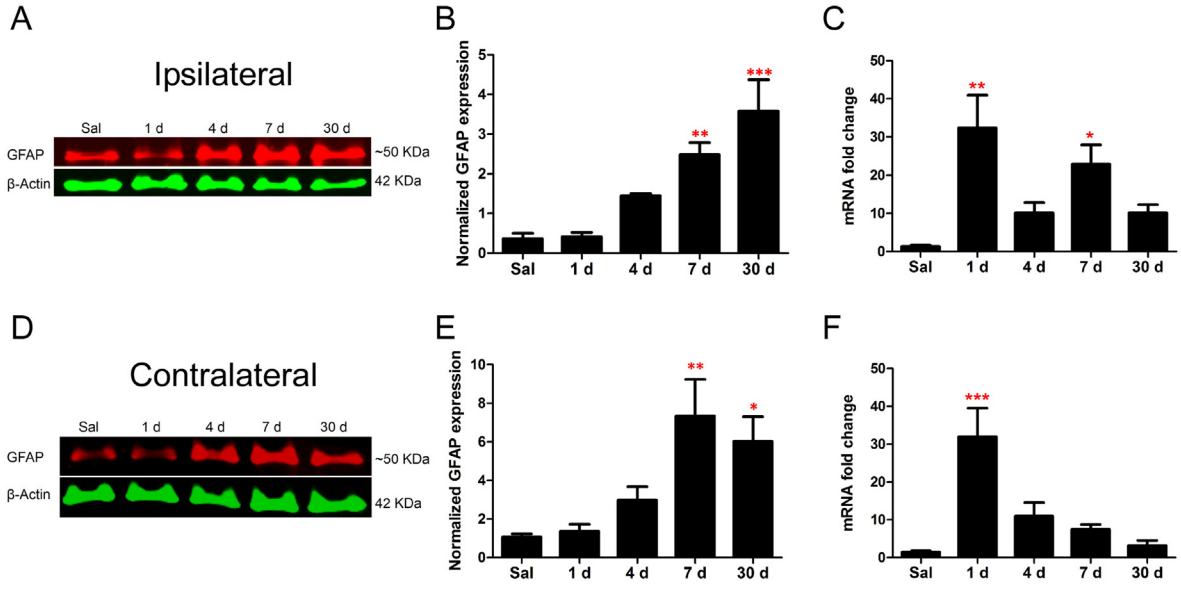

Fig. 2. Hippocampal protein and mRNA quantification of glial fibrillary acidic protein (GFAP) after kainic acid-induced status epilepticus (SE). A. Representative Western blot of GFAP (red) and β-actin (green) protein from the ipsilateral hippocampus of a saline control (Sal) and 1, 4, 7, and 30 days (d) after kainic acid-induced SE. B. Quantification of GFAP band intensities normalized to β-actin at each time point in the ipsilateral hippocampus. C. Fold change in GFAP mRNA levels in the ipsilateral hippocampal tissue from saline controls (Sal) and in tissue collected 1, 4, 7, and 30 days (d) post SE. D. Representative Western blot of GFAP (red) and β-actin (green) protein from the contralateral hippocampus from a saline control (Sal) and 1, 4, 7, and 30 days (d) post SE. E. Quantification of contralateral GFAP protein normalized to β-actin in each group. F. Quantification of GFAP mRNA levels in the contralateral hippocampus of saline controls (Sal) and various time points post SE. * indicates $p < 0.05$, ** indicates $p < 0.01$, and *** indicates $p < 0.001$ when compared to saline control and $n = 5$ for each time point.

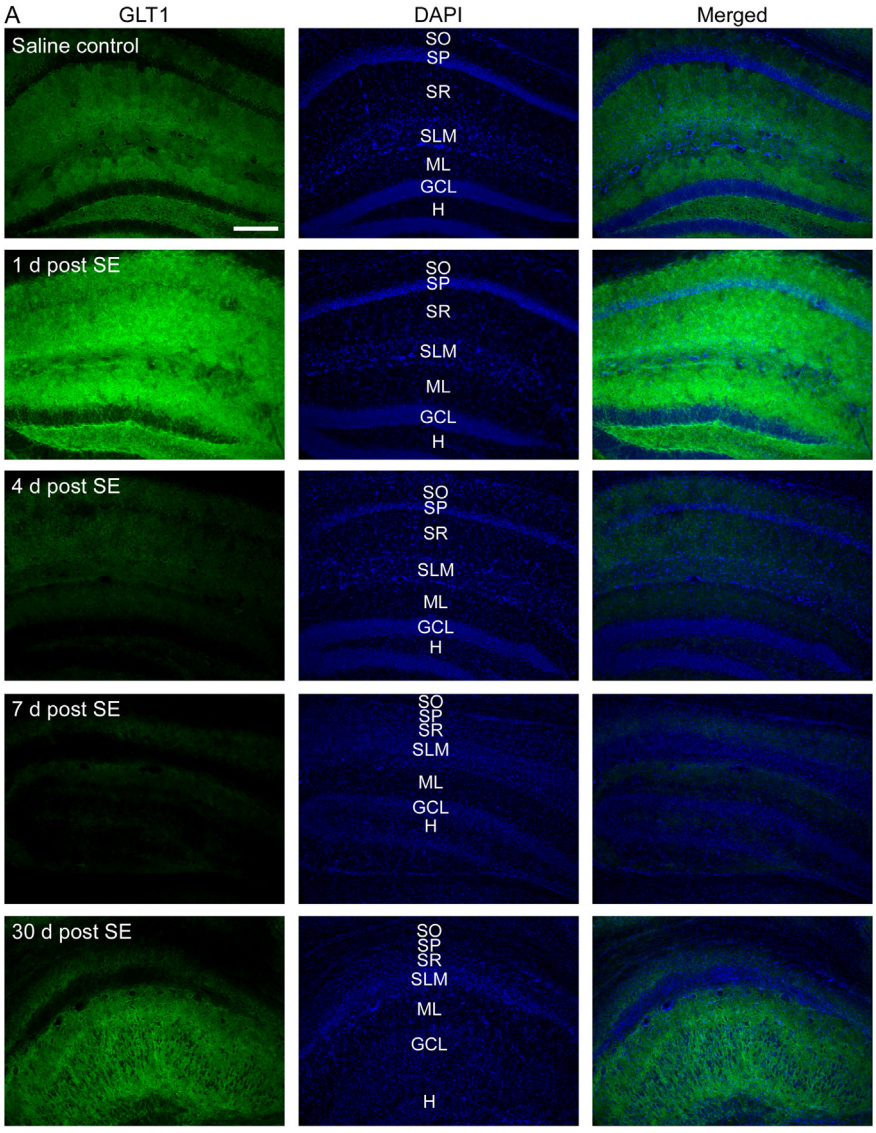

Fig. 3. Glutamate transporter-1 (GLT1) immunoreactivity in the ipsilateral hippocampus after kainic acid-induced status epilepticus (SE). A. 10× images of GLT1 (green), DAPI (blue), and merged immunoreactivity of the ipsilateral hippocampus after saline injections (Saline control) and 1, 4, 7, and 30 days (d) post SE. B. Quantification of GLT1 immunoreactivity in the various layers of the hippocampus ipsilateral to kainic acid injections. * indicates $p < 0.05$, ** indicates $p < 0.01$, and *** indicates $p < 0.001$ when compared to saline control. Scale bar = 200 μm. SO = stratum oriens; SP = stratum pyramidale; SR = stratum radiatum; SLM = stratum lacunosum moleculare; ML = molecular layer; GCL = granule cell layer; H = hilus.

3.3. Changes in aquaporin-4 (AQP4) expression

We have previously demonstrated marked downregulation of AQP4 immunoreactivity in the IHKA model (Lee et al., 2012b). Therefore, we aimed to characterize AQP4 protein and mRNA expression changes using Western blot and RT-PCR, respectively. We found a dramatic downregulation of AQP4 protein 1 day and 4 days post SE in the ipsilateral dorsal hippocampus (Fig. 6A–B). AQP4 returned to nearly control protein levels by 7 days post SE and significantly increased AQP4 protein levels were observed at 30 days post SE. In the contralateral dorsal hippocampus, AQP4 protein was immediately downregulated by 1 day post SE (Fi. 6D-E). This was followed by a gradual return to control AQP4 levels. Increased levels of AQP4 mRNA were observed 7 days post SE in both the ipsilateral (Fig. 6C) and contralateral (Fig. 6F) dorsal hippocampi. The highest level of AQP4 mRNA expression, however, was observed 4 days post SE in the ipsilateral dorsal hippocampus. Together, these results suggest that AQP4 regulation in the dorsal hippocampus occurs both at the mRNA and protein level in the IHKA model of epilepsy. Separate analysis of whole hippocampal AQP4 protein revealed no changes at any time point examined (Supplemental Fig. S10 in the online version at http://dx.doi.org/10.1016/j.expneurol.2016.05.003.); AQP4 mRNA levels, however, were significantly increased in both the ipsilateral and contralateral hippocampi to injection (Supplemental Fig. S10 in the online version at http://dx.doi.org/10.1016/j.expneurol.2016.05.003.).

4. Discussion

In this study, we used RT-PCR, Western blot, and immunohistochemistry to examine changes in the key astrocytic molecules GFAP, GLT1, and AQP4 at various time points post status epilepticus (SE) in the intrahippocampal kainic acid (IHKA) model of epilepsy. First, we found pronounced increases in GFAP immunoreactivity and hippocampal GFAP protein levels accompanied by transient increases in GFAP mRNA. Second, we found an upregulation of dorsal hippocampal GLT1 immunoreactivity and protein at 1 day post SE. Third, we found a significant reduction in dorsal hippocampal GLT1 immunoreactivity and protein expression at 4 and 7 days post SE, which returned to near control

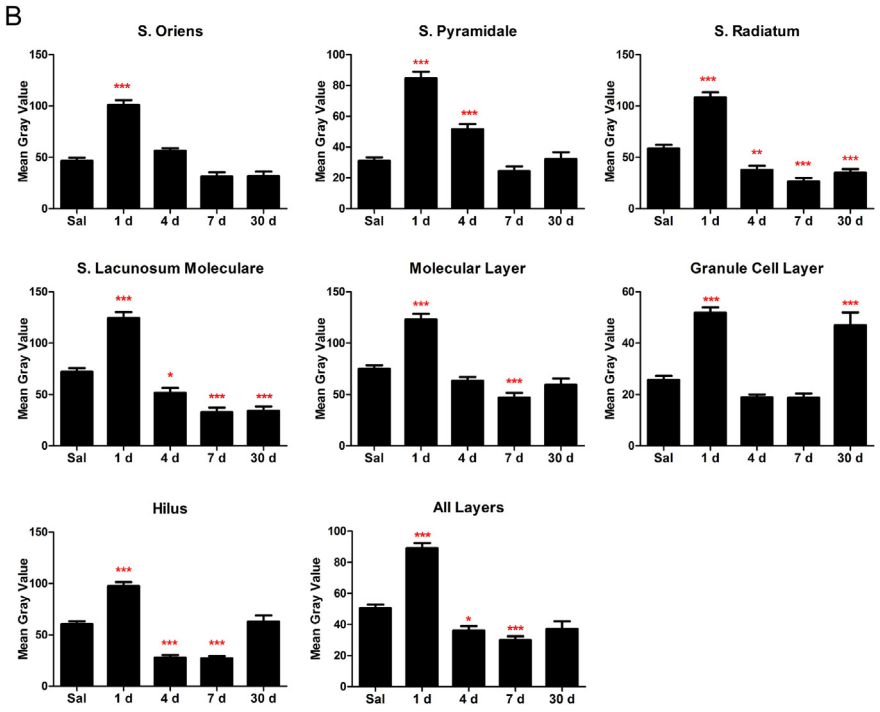

Fig. 3 (*continued*).

levels by 30 days post SE. Fourth, AQP4 dorsal hippocampal protein levels were immediately downregulated and mRNA upregulated shortly after kainic acid-induced SE. Fifth, we found significant regulation of GLT1 and AQP4 in the hippocampus contralateral as well as ipsilateral to KA injection; interestingly, these changes occurred in the absence of sclerotic changes (such as CA1 pyramidal cell death and dentate granule cell dispersion) in the contralateral hippocampus. Thus, regulation of AQP4 and GLT1 by seizure activity does not appear to require cell death/sclerosis. This time course study is the first to examine mRNA, protein, and immunoreactivity changes of GLT1 and AQP4 in a well-established model of temporal lobe epilepsy (TLE). These results support the hypothesis that intense seizures regulate GLT1 and AQP4 expression and may lead to a functionally relevant astrocytic dysregulation of glutamate uptake and water and potassium homeostasis during epileptogenesis.

4.1. Increased GFAP expression following SE

Hippocampal sclerosis (HS), a common pathological feature of TLE, is characterized by a pronounced loss of pyramidal neurons, granule cell dispersion, microvascular proliferation, synaptic reorganization, and reactive gliosis (Blümcke et al., 1999; Clasadonte and Haydon, 2012; de Lanerolle et al., 2012; Margerison and Corsellis, 1966). When present, the sclerotic hippocampus may be the focus of seizure origin (Babb et al., 1984). Here, we used GFAP, a member of the intermediate filament structural protein family that is predominantly expressed by astrocytes, as a marker for astrocytic gliosis (astrogliosis). Similar to what was observed previously in the contralateral hippocampus (Lee et al., 2012b), a progressive increase in GFAP immunoreactivity over time was detected in the hippocampus ipsilateral to intrahippocampal kainic acid (IHKA) injections. The most prominent levels were observed at the 30 days post SE when the ipsilateral hippocampus exhibited signs of HS (including granule cell dispersion, CA1 cell loss and reactive astrocytosis). Parallel to these observations, we found progressive increases in GFAP protein levels over time. Early significant upregulation of GFAP mRNA was observed at 1 day, most likely contributing to the protein increases. Similar to our results, other studies have also found significant increases in GFAP gene expression in both the latent and chronic stages of epilepsy (Lukasiuk and Pitkänen, 2004). Our findings also match previous studies that demonstrated increased GFAP expression in the electrical kindling (Miyazaki et al., 2003; Stringer, 1996; Torre et al., 1993), pentylenetetrazol (PTZ) (Torre et al., 1993), kainic acid (Bendotti et al., 2000; Lee et al., 2012b), and frequent repetitive febrile seizures (FRFS) (Yang et al., 2009) models of epilepsy.

Although astrogliosis in epilepsy is well established, the mechanism of GFAP upregulation remains unknown. One study has suggested transcriptional activation of GFAP by the neuropeptide galanin and calcitonin gene-related peptide (CGRP) in cultured astrocytes (Priller et al., 1998). More recently, it was observed that IL-1β regulated cortical reorganization of F-actin through Rho GTPase-Rho kinase pathway (John et al., 2004). In a murine corticectomy model of CNS lesion, GFAP transcript elevation immediately followed the early rise in IL-1β mRNA (Herx and Yong, 2001). Interestingly, IL-1β knockout mice did not exhibit injury-induced upregulation of GFAP mRNA and protein 2–3 days after injury, although GFAP immunoreactivity was not different between wild-type and knockout mice by 5–7 days after lesion induction (Herx and Yong, 2001). Future studies could further elucidate mechanisms of GFAP upregulation. Whether astrogliosis itself contributes to epileptogenesis is unclear. A recent study has shown that mice with conditional deletion of β1-integrin develop widespread reactive astrogliosis, spontaneous seizures and impairment of glutamate uptake (Robel et al., 2015).

4.2. Pronounced glutamate transporter-1 (GLT1) expression changes following SE

It is well known that extracellular levels of glutamate are elevated during seizures (Campbell and Hablitz, 2004; During and Spencer, 1993; Glass and Dragunow, 1995; Hubbard et al., 2013; Tanaka et al., 1997). Increased levels of glutamate in the extracellular space (ECS) are likely due either to increased glutamate release and/or impaired reuptake. Glutamate transporter-1 (GLT1) is responsible for the majority of glutamate uptake from the ECS (Danbolt, 2001) and therefore reduced levels of glutamate uptake by GLT1 could powerfully contribute to hyperexcitability and seizure generation.

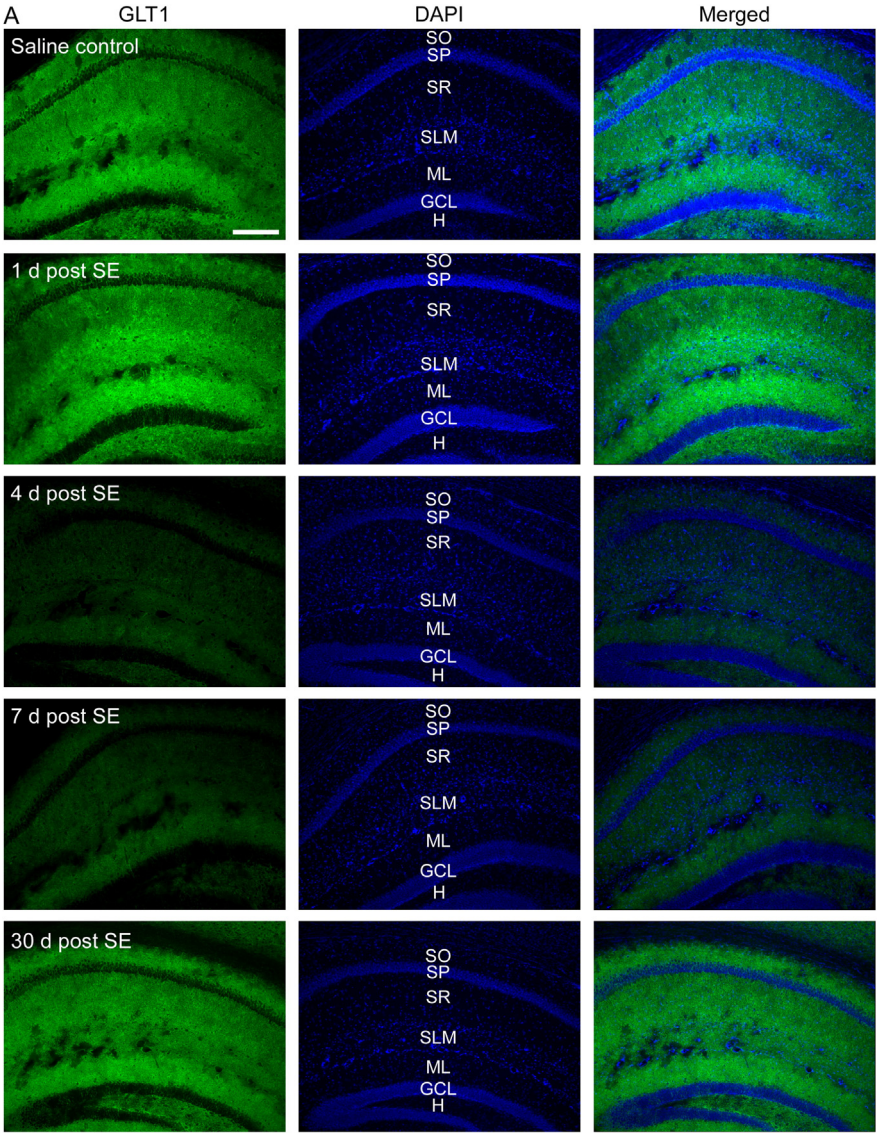

Fig. 4. Glutamate transporter-1 (GLT1) immunoreactivity in the contralateral hippocampus after kainic acid-induced status epilepticus (SE). A. 10× images of GLT1 (green), DAPI (blue), and merged immunoreactivity of the contralateral hippocampus after saline injections (Saline control) and 1, 4, 7, and 30 days (d) post SE. B. Quantification of GLT1 immunoreactivity in the various layers of the hippocampus contralateral to kainic acid injections. * indicates $p < 0.05$, ** indicates $p < 0.01$, and *** indicates $p < 0.001$ when compared to saline control. Scale bar = 200 μm. SO = stratum oriens; SP = stratum pyramidale; SR = stratum radiatum; SLM = stratum lacunosum moleculare; ML = molecular layer; GCL = granule cell layer; H = hilus.

Human tissue data have revealed reduced GLT1 (human analog is called excitatory amino acid transporter 2, EAAT2) immunoreactivity in the sclerotic hippocampus (Mathern et al., 1999; Proper et al., 2002; van der Hel et al., 2005) and either no change (Mathern et al., 1999) or increased GLT1/EAAT2 expression in the non-HS (Bjornsen et al., 2007; Eid et al., 2004; Tessler et al., 1999). The use of animal models, on the other hand, has so far demonstrated equivocal results on the regulation of GLT1 expression in epilepsy. Downregulation (Samuelsson et al. 2000; Ueda et al. 2001; Lopes et al. 2013; Sakurai et al., 2015), upregulation (Simantov et al. 1999), or no change (Miller et al. 1997) in GLT1 have all been reported in a variety of epilepsy models. These differences, however, can be accounted for by several factors, including mRNA *vs.* protein evaluation, distinct models used, brain region examined, and time point(s) used in the study (*e.g.*, latent or chronic phase). For example, we demonstrated an initial increase in GLT1 expression that subsided and subsequently became downregulated in the dorsal hippocampus. Our current study is the first to examine both early and chronic time points, regional specificity (dorsal *vs.* whole hippocampus and hippocampal field and laminar analysis), and combine immunoreactivity with Western blot and RT-PCR analysis.

Recent studies have shown dynamic regulation of astrocyte GLT1. Recently, Sakurai et al. (2015) demonstrated that neuronal cell death was associated with a focal loss of GLT1 immunoreactivity and stronger immunoreactivity for glutamate (Sakurai et al., 2015). In addition, Murphy-Royal et al. (2015) found that although GLT1 is anchored to the membrane at synapses, it can be untethered after glutamate release and can undergo rapid, activity-regulated surface diffusion between synaptic and non-synaptic sites to ensure effective glutamate clearance (Murphy-Royal et al., 2015). Since GLT1 may be regulated by the intensity of neuronal activity, its expression may vary during the course of epileptogenesis, as we have shown here. Increased levels were found at 1 day post SE (after a long duration of high intensity seizures) with decreased levels becoming apparent as early as 4 days post SE. The early reduction of GLT1 expression may lead to increased extracellular glutamate levels that consequently contribute to hyperexcitability and neuronal cell death. The loss of GLT1, therefore, could contribute to

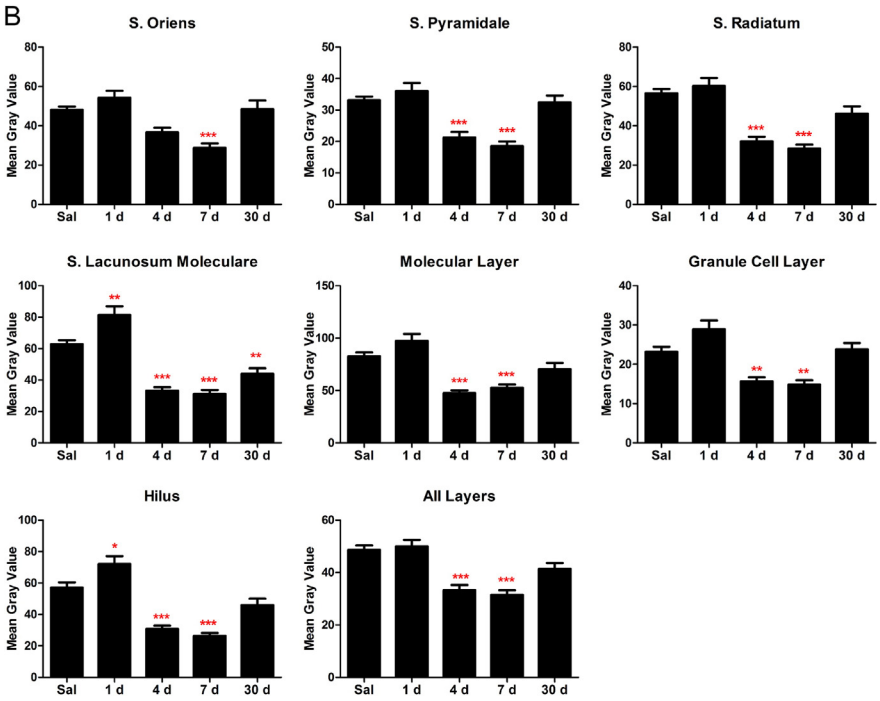

Fig. 4 (*continued*).

the transition from a healthy brain to an epileptic one. Further studies will need to characterize (i) mechanisms of regulation of GLT1 by seizures; (ii) subcellular trafficking of GLT1; and (iii) posttranslational modification(s) of GLT1 in epilepsy. Posttranslational modifications such as sumoylation (Foran et al., 2014) and S-nitrosylation (Raju et al., 2015) have been described that may contribute to alterations in plasma membrane *vs.* cytosolic localization of GLT1. Subcellular trafficking of GLT1 would carry significant implications for the efficacy of glutamate clearance and thus network hyperexcitability.

4.3. Striking aquaporin-4 (AQP4) changes following SE

Increasing evidence suggests dysregulation of water and potassium homeostasis in epilepsy (Binder et al., 2012; Binder and Steinhäuser, 2006). Expression and subcellular localization of AQP4 is altered in sclerotic human hippocampi (Lee et al., 2004), with increased total AQP4 protein but a reduction in perivascular membrane expression (Eid et al., 2005). AQP4 knockout mice have significantly prolonged seizure duration associated with a deficit in extracellular K^+ clearance (Binder et al., 2006; Haj-Yasein et al., 2015; Strohschein et al., 2011). These results together suggest a pro-epileptogenic effect of AQP4 dysregulation (Binder et al., 2012; Dudek and Rogawski, 2005; Wetherington et al., 2008). In the current study, we found decreased dorsal AQP4 protein levels in both the ipsilateral and contralateral dorsal hippocampi 1 day post SE. These results closely align with previously observed reductions in AQP4 immunoreactivity early after SE (Lee et al., 2012b). In the dorsal ipsilateral hippocampus, AQP4 protein levels remained downregulated at 4 days post SE and were found to be upregulated in the chronically epileptic brain (30 days post SE). We also found transient increases in AQP4 mRNA levels. These mRNA changes may be compensatory, restoring AQP4 protein levels after the significant drop in protein at early time points post SE.

Other results also suggest that AQP4 dysregulation may occur early during epileptogenesis. Kim et al. studied regulation of various aquaporins in the rat pilocarpine model of epilepsy (Kim et al., 2009; Kim et al., 2010). In control animals, AQP4 immunoreactivity was detected diffusely in the piriform cortex and hippocampus, with the greatest expression at astrocyte endfeet. Following status epilepticus in this model the authors describe an "AQP4-deleted area" in the piriform cortex. However, EEG analysis for timing of spontaneous seizure onset was not investigated. In a distinct model of intraperitoneal kainic acid administration in rats, Alvestad et al. (2013) found mislocalization of AQP4. In particular, using immunogold analysis these investigators demonstrated that AQP4 was reduced in adluminal endfoot membranes but was stable or slightly increased in abluminal endfoot membranes (Alvestad et al., 2013). This occurred in the early epileptogenic period prior to the occurrence of spontaneous seizures. AQP4 regulation and subcellular compartmentalization remain to be examined in other models of epilepsy. In particular, distinct epilepsy models in which epileptogenesis occurs in the *absence* of detectable cell death would prove useful in determining the threshold for AQP4 regulation.

Alterations in glial molecules during epileptogenesis may play a role in epilepsy-associated cognitive dysfunction. For example, increasing evidence has suggested an important role for AQP4 in the regulation of synaptic plasticity in the hippocampus and amygdala (Szu and Binder, 2016). AQP4-deficient mice have been found to have marked deficits in synaptic plasticity, including deficits in long-term potentiation and long-term depression, and impairment in location-specific object memory (Skucas et al., 2011). More recent studies from other groups have confirmed deficits in synaptic plasticity in AQP4-deficient mice (Fan et al., 2013; Li et al., 2012; Yang et al., 2013). In human patients with mesial TLE, a correlation between IQ and AQP4 expression was observed (Kandratavicius et al., 2015). Therefore, a downregulation of AQP4 may lead not only to hyperexcitability but also to broader deficits in synaptic plasticity and cognitive performance which are important comorbidities in patients with epilepsy (Bell et al., 2011; Brooks-Kayal et al., 2013).

5. Conclusion

Here we demonstrate reductions in GLT1 and AQP4 during the early epileptogenic period. Early disruption of astrocytic water, potassium, and glutamate homeostasis could have powerful epileptogenic and cognitive effects. While there is some apparent partial recovery of overall

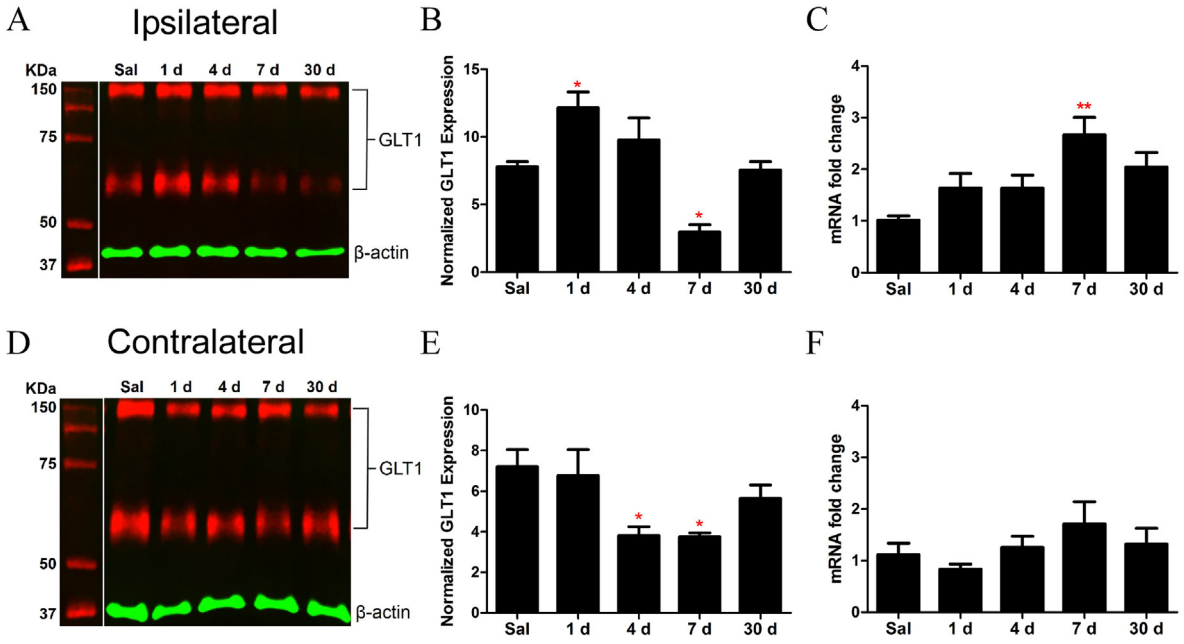

Fig. 5. Dorsal hippocampal glutamate transporter-1 (GLT1) protein and mRNA levels after kainic acid-induced status epilepticus (SE). A. Representative Western blot of GLT1 (red) and β-actin (green) protein from the ipsilateral hippocampus of a saline control (Sal) and 1, 4, 7, and 30 days (d) post kainic acid-induced SE. B. Quantification of GLT1 lower band intensity normalized to β-actin at each time point in the ipsilateral hippocampus. C. Fold change in GLT1 mRNA in the ipsilateral hippocampus from tissue collected from saline controls (Sal) and at 1, 4, 7, and 30 days (d) post kainic acid-induced SE. D. Representative Western blot of GLT1 (red) and β-actin (green) protein from the contralateral hippocampus of a saline control (Sal) and 1, 4, 7, and 30 days post SE. E. Quantification of contralateral hippocampal GLT1 lower protein band normalized to β-actin in each group. F. Quantification of GLT1 mRNA levels in the contralateral hippocampus from tissue collected from saline controls (Sal) and at various time points post kainic acid-induced SE. * indicates $p < 0.05$ and ** indicates $p < 0.01$ when compared to saline control. For each time point, $n = 5$ except protein for 7 days post SE ($n = 7$).

AQP4 and GLT1 expression at the longest time point studied (30 days), the pattern of expression remains quite distinct, and subcellular dysregulation of AQP4 function is known to occur in chronic epilepsy (Alvestad et al., 2013; Eid et al., 2005). Furthermore, in addition to these changes in key astrocyte molecules, the overall anatomy of the hippocampus changes dramatically in the progression toward hippocampal sclerosis. Future studies could examine mechanisms of activity-regulated GLT1 and AQP4 expression *in vitro* and *in vivo*. In addition, if normalization of GLT1 and AQP4 expression and function ameliorates hyperexcitability, this could provide a new astrocyte-based antiepileptogenic strategy.

Supplementary data to this article can be found online at http://dx.doi.org/10.1016/j.expneurol.2016.05.003.

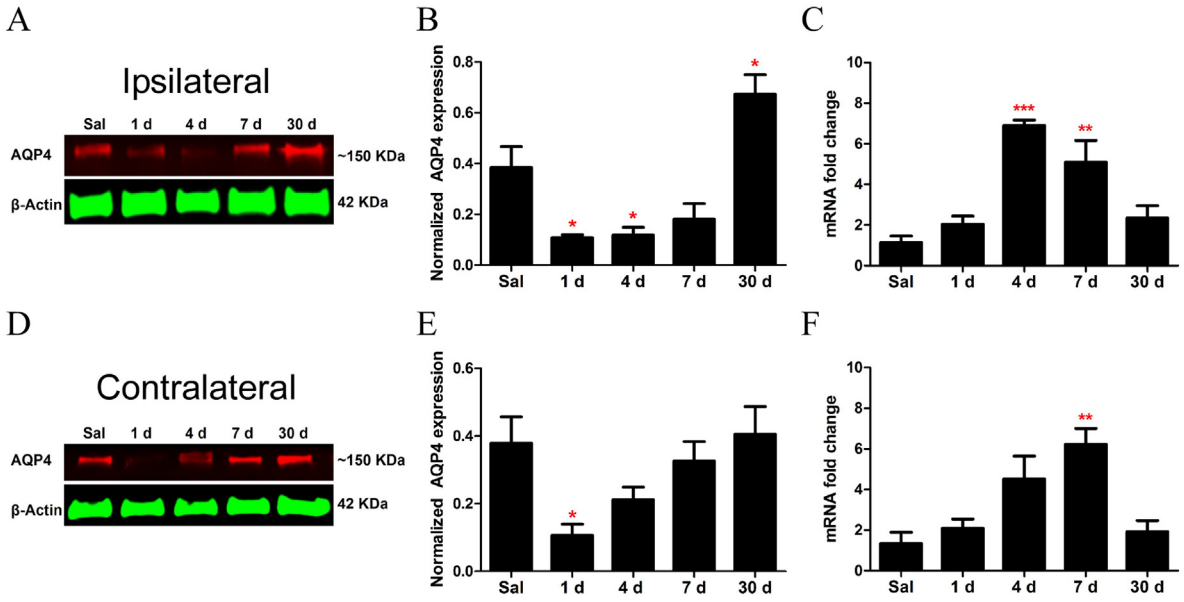

Fig. 6. Dorsal hippocampal aquaporin-4 (AQP4) protein and mRNA levels after kainic acid-induced status epilepticus (SE). A. Representative Western blot of AQP4 (red) and β-actin (green) protein from the ipsilateral hippocampus from a saline control (Sal) and 1, 4, 7, and 30 days (d) post SE. B. Quantification of AQP4 band intensities normalized to β-actin at each time point from the ipsilateral hippocampus. C. Fold change in AQP4 mRNA in the ipsilateral hippocampus from saline controls (Sal) and 1, 4, 7, and 30 days (d) post SE. D. Representative Western blot of AQP4 (red) and β-actin (green) protein from the contralateral hippocampus in a saline control (Sal) and 1, 4, 7, and 30 days post kainic acid-induced SE. E. Quantification of AQP4 protein from the contralateral hippocampus normalized to β-actin in each group. F. Quantification of AQP4 mRNA levels in the contralateral hippocampus in tissue collected from saline controls (Sal) and at various time points post SE. * indicates $p < 0.05$, ** indicates $p < 0.01$, and *** indicates $p < 0.001$ when compared to saline control and $n = 5$ for each time point.

Acknowledgments

This work was supported by NIH RO1 grants NS082570 and NS081243 to DKB. The authors would like to thank Dr. Emma Wilson (UCR) for the use of her Leica DFC345 FX fluorescence microscope, Dr. Michael Robinson (UPENN) for the provision of the C-terminal polyclonal antibody to GLT1 used in these studies, and Andrew Nakla for his assistance with Western blots.

References

Agre, P., King, L.S., Yasui, M., Guggino, W.B., Ottersen, O.P., Fujiyoshi, Y., Engel, A., Nielsen, S., 2002. Aquaporin water channels—from atomic structure to clinical medicine. J. Physiol. 542, 3–16.

Alvestad, S., Hammer, J., Hoddevik, E.H., Skare, O., Sonnewald, U., Amiry-Moghaddam, M., Ottersen, O.P., 2013. Mislocalization of AQP4 precedes chronic seizures in the kainate model of temporal lobe epilepsy. Epilepsy Res. 105, 30–41.

Amiry-Moghaddam, M., Ottersen, O.P., 2003. The molecular basis of water transport in the brain. Nat. Rev. Neurosci. 4, 991–1001.

Arabadzisz, D., Antal, K., Parpan, F., Emri, Z., Fritschy, J.M., 2005. Epileptogenesis and chronic seizures in a mouse model of temporal lobe epilepsy are associated with distinct EEG patterns and selective neurochemical alterations in the contralateral hippocampus. Exp. Neurol. 194, 76–90.

Araque, A., Parpura, V., Sanzgiri, R.P., Haydon, P.G., 1999. Tripartite synapses: glia, the unacknowledged partner. Trends Neurosci. 22, 208–215.

Babb, T.L., Lieb, J.P., Brown, W.J., Pretorius, J., Crandall, P.H., 1984. Distribution of pyramidal cell density and hyperexcitability in the epileptic human hippocampal formation. Epilepsia 25, 721–728.

Bell, B., Lin, J.J., Seidenberg, M., Hermann, B., 2011. The neurobiology of cognitive disorders in temporal lobe epilepsy. Nat. Rev. Neurol. 7, 154–164.

Bendotti, C., Guglielmetti, F., Tortarolo, M., Samanin, R., Hirst, W.D., 2000. Differential expression of S100beta and glial fibrillary acidic protein in the hippocampus after kainic acid-induced lesions and mossy fiber sprouting in adult rat. Exp. Neurol. 161, 317–329.

Binder, D.K., Nagelhus, E.A., Ottersen, O.P., 2012. Aquaporin-4 and epilepsy. Glia 60, 1203–1214.

Binder, D.K., Papadopoulos, M.C., Haggie, P.M., Verkman, A.S., 2004. In vivo measurement of brain extracellular space diffusion by cortical surface photobleaching. J. Neurosci. 24, 8049–8056.

Binder, D.K., Steinhäuser, C., 2006. Functional changes in astroglial cells in epilepsy. Glia 54, 358–368.

Binder, D.K., Yao, X., Zador, Z., Sick, T.J., Verkman, A.S., Manley, G.T., 2006. Increased seizure duration and slowed potassium kinetics in mice lacking aquaporin-4 water channels. Glia 53, 631–636.

Bjornsen, L.P., Eid, T., Holmseth, S., Danbolt, N.C., Spencer, D.D., de Lanerolle, N.C., 2007. Changes in glial glutamate transporters in human epileptogenic hippocampus: inadequate explanation for high extracellular glutamate during seizures. Neurobiol. Dis. 25, 319–330.

Blümcke, I., Beck, H., Lie, A.A., Wiestler, O.D., 1999. Molecular neuropathology of human mesial temporal lobe epilepsy. Epilepsy Res. 36, 205–223.

Bouilleret, V., Ridoux, V., Depaulis, A., Marescaux, C., Nehlig, A., Le Gal La Salle, G., 1999. Recurrent seizures and hippocampal sclerosis following intrahippocampal kainate injection in adult mice: electroencephalography, histopathology and synaptic reorganization similar to mesial temporal lobe epilepsy. Neuroscience 89, 717–729.

Brooks-Kayal, A.R., Bath, K.G., Berg, A.T., Galanopoulou, A.S., Holmes, G.L., Jensen, F.E., Kanner, A.M., O'Brien, T.J., Whittemore, V.H., Winawer, M.R., Patel, M., Scharfman, H.E., 2013. Issues related to symptomatic and disease-modifying treatments affecting cognitive and neuropsychiatric comorbidities of epilepsy. Epilepsia 54 (Suppl. 4), 44–60.

Campbell, S.L., Hablitz, J.J., 2004. Glutamate transporters regulate excitability in local networks in rat neocortex. Neuroscience 127, 625–635.

Clasadonte, J., Haydon, P.G., 2012. Astrocytes and Epilepsy. In: Noebels, J.L., Avoli, M., Rogawski, M.A., Olsen, R.W., Delgado-Escueta, A.V. (Eds.), Jasper's Basic Mechanisms of the Epilepsies, fourth ed. Bethesda (MD).

Danbolt, N.C., 2001. Glutamate uptake. Prog. Neurobiol. 65, 1–105.

de Lanerolle, N.C., Lee, T.S., Spencer, D.D., 2012. Histopathology of Human Epilepsy. In: Noebels, J.L., Avoli, M., Rogawski, M.A., Olsen, R.W., Delgado-Escueta, A.V. (Eds.), Jasper's Basic Mechanisms of the Epilepsies, fourth ed. Bethesda (MD).

Dudek, F.E., Rogawski, M.A., 2005. Regulation of brain water: is there a role for aquaporins in epilepsy? Epilepsy Curr. 5, 104–106.

During, M.J., Spencer, D.D., 1993. Extracellular hippocampal glutamate and spontaneous seizure in the conscious human brain. Lancet 341, 1607–1610.

Eid, T., Lee, T.S., Thomas, M.J., Amiry-Moghaddam, M., Bjornsen, L.P., Spencer, D.D., Agre, P., Ottersen, O.P., de Lanerolle, N.C., 2005. Loss of perivascular aquaporin-4 may underlie deficient water and K^+ homeostasis in the human epileptogenic hippocampus. Proc. Natl. Acad. Sci. U. S. A. 102, 1193–1198.

Eid, T., Thomas, M.J., Spencer, D.D., Runden-Pran, E., Lai, J.C., Malthankar, G.V., Kim, J.H., Danbolt, N.C., Ottersen, O.P., de Lanerolle, N.C., 2004. Loss of glutamine synthetase in the human epileptogenic hippocampus: possible mechanism for raised extracellular glutamate in mesial temporal lobe epilepsy. Lancet 363, 28–37.

Fan, Y., Liu, M., Wu, X., Wang, F., Ding, J., Chen, J., Hu, G., 2013. Aquaporin-4 promotes memory consolidation in Morris water maze. Brain Struct. Funct. 218, 39–50.

Foran, E., Rosenblum, L., Bogush, A., Pasinelli, P., Trotti, D., 2014. Sumoylation of the astroglial glutamate transporter EAAT2 governs its intracellular compartmentalization. Glia 62, 1241–1253.

Glass, M., Dragunow, M., 1995. Neurochemical and morphological changes associated with human epilepsy. Brain Res. Brain Res. Rev. 21, 29–41.

Haj-Yasein, N.N., Bugge, C.E., Jensen, V., Ostby, I., Ottersen, O.P., Hvalby, O., Nagelhus, E.A., 2015. Deletion of aquaporin-4 increases extracellular K(+) concentration during synaptic stimulation in mouse hippocampus. Brain Struct. Funct. 220, 2469–2474.

Halassa, M.M., Haydon, P.G., 2010. Integrated brain circuits: astrocytic networks modulate neuronal activity and behavior. Annu. Rev. Physiol. 72, 335–355.

Herx, L.M., Yong, V.W., 2001. Interleukin-1 beta is required for the early evolution of reactive astrogliosis following CNS lesion. J. Neuropathol. Exp. Neurol. 60, 961–971.

Hesdorffer, D.C., Logroscino, G., Benn, E.K., Katri, N., Cascino, G., Hauser, W.A., 2011. Estimating risk for developing epilepsy: a population-based study in Rochester, Minnesota. Neurology 76, 23–27.

Hubbard, J.A., Hsu, M.S., Fiacco, T.A., Binder, D.K., 2013. Glial cell changes in epilepsy: overview of the clinical problem and therapeutic opportunities. Neurochem. Int. 63, 638–651.

John, G.R., Chen, L., Rivieccio, M.A., Melendez-Vasquez, C.V., Hartley, A., Brosnan, C.F., 2004. Interleukin-1beta induces a reactive astroglial phenotype via deactivation of the Rho GTPase-Rock axis. J. Neurosci. 24, 2837–2845.

Kandratavicius, L., Peixoto-Santos, J.E., Monteiro, M.R., Scandiuzzi, R.C., Carlotti Jr., C.G., Assirati Jr., J.A., Hallak, J.E., Leite, J.P., 2015. Mesial temporal lobe epilepsy with psychiatric comorbidities: a place for differential neuroinflammatory interplay. J. Neuroinflammation 12, 38.

Kim, J.E., Ryu, H.J., Yeo, S.I., Seo, C.H., Lee, B.C., Choi, I.G., Kim, D.S., Kang, T.C., 2009. Differential expressions of aquaporin subtypes in astroglia in the hippocampus of chronic epileptic rats. Neuroscience 163, 781–789.

Kim, J.E., Yeo, S.I., Ryu, H.J., Kim, M.J., Kim, D.S., Jo, S.M., Kang, T.C., 2010. Astroglial loss and edema formation in the rat piriform cortex and hippocampus following pilocarpine-induced status epilepticus. J. Comp. Neurol. 518, 4612–4628.

Kong, Q., Takahashi, K., Schulte, D., Stouffer, N., Lin, Y., Lin, C.L., 2012. Increased glial glutamate transporter EAAT2 expression reduces epileptogenic processes following pilocarpine-induced status epilepticus. Neurobiol. Dis. 47, 145–154.

Lee, D.J., Amini, M., Hamamura, M.J., Hsu, M.S., Seldin, M.M., Nalcioglu, O., Binder, D.K., 2012a. Aquaporin-4-dependent edema clearance following status epilepticus. Epilepsy Res. 98, 264–268.

Lee, D.J., Hsu, M.S., Seldin, M.M., Arellano, J.L., Binder, D.K., 2012b. Decreased expression of the glial water channel aquaporin-4 in the intrahippocampal kainic acid model of epileptogenesis. Exp. Neurol. 235, 246–255.

Lee, T.S., Eid, T., Mane, S., Kim, J.H., Spencer, D.D., Ottersen, O.P., de Lanerolle, N.C., 2004. Aquaporin-4 is increased in the sclerotic hippocampus in human temporal lobe epilepsy. Acta Neuropathol. 108, 493–502.

Li, Y.K., Wang, F., Wang, W., Luo, Y., Wu, P.F., Xiao, J.L., Hu, Z.L., Jin, Y., Hu, G., Chen, J.G., 2012. Aquaporin-4 deficiency impairs synaptic plasticity and associative fear memory in the lateral amygdala: involvement of downregulation of glutamate transporter-1 expression. Neuropsychopharmacology 37, 1867–1878.

Lopes, M.W., Soares, F.M., de Mello, N., Nunes, J.C., Cajado, A.G., de Brito, D., de Cordova, F.M., da Cunha, R.M., Walz, R., Leal, R.B., 2013. Time-dependent modulation of AMPA receptor phosphorylation and mRNA expression of NMDA receptors and glial glutamate transporters in the rat hippocampus and cerebral cortex in a pilocarpine model of epilepsy. Exp. Brain Res. 226 (2), 153–163.

Lukasiuk, K., Pitkänen, A., 2004. Large-scale analysis of gene expression in epilepsy research: is synthesis already possible? Neurochem. Res. 29, 1169–1178.

Ma, T., Yang, B., Gillespie, A., Carlson, E.J., Epstein, C.J., Verkman, A.S., 1997. Generation and phenotype of a transgenic knockout mouse lacking the mercurial-insensitive water channel aquaporin-4. J. Clin. Invest. 100, 957–962.

Margerison, J.H., Corsellis, J.A., 1966. Epilepsy and the temporal lobes. A clinical, electroencephalographic and neuropathological study of the brain in epilepsy, with particular reference to the temporal lobes. Brain 89, 499–530.

Mathern, G.W., Mendoza, D., Lozada, A., Pretorius, J.K., Dehnes, Y., Danbolt, N.C., Nelson, N., Leite, J.P., Chimelli, L., Born, D.E., Sakamoto, A.C., Assirati, J.A., Fried, I., Peacock, W.J., Ojemann, G.A., Adelson, P.D., 1999. Hippocampal GABA and glutamate transporter immunoreactivity in patients with temporal lobe epilepsy. Neurology 52, 453–472.

Miller, H.P., Levey, A.I., Rothstein, J.D., Tzingounis, A.V., Conn, P.J., 1997. Alterations in glutamate transporter protein levels in kindling-induced epilepsy. J. Neurochem. 68 (4), 1564–1570.

Miyazaki, T., Miyamoto, O., Janjua, N.A., Hata, T., Takahashi, F., Itano, T., 2003. Reactive gliosis in areas around third ventricle in association with epileptogenesis in amygdaloid-kindled rat. Epilepsy Res. 56, 5–15.

Murphy-Royal, C., Dupuis, J.P., Varela, J.A., Panatier, A., Pinson, B., Baufreton, J., Groc, L., Oliet, S.H., 2015. Surface diffusion of astrocytic glutamate transporters shapes synaptic transmission. Nat. Neurosci. 18, 219–226.

Nagelhus, E.A., Mathiisen, T.M., Ottersen, O.P., 2004. Aquaporin-4 in the central nervous system: cellular and subcellular distribution and coexpression with KIR4.1. Neuroscience 129, 905–913.

Nielsen, S., Nagelhus, E.A., Amiry-Moghaddam, M., Bourque, C., Agre, P., Ottersen, O.P., 1997. Specialized membrane domains for water transport in glial cells: high-resolution immunogold cytochemistry of aquaporin-4 in rat brain. J. Neurosci. 17, 171–180.

Paxinos, G., Franklin, K.B.J., 2001. The mouse brain in stereotaxic coordinates. second ed. Academic Press, San Diego, CA.

Priller, J., Haas, C.A., Reddington, M., Kreutzberg, G.W., 1998. Cultured astrocytes express functional receptors for galanin. Glia 24, 323–328.

Proper, E.A., Hoogland, G., Kappen, S.M., Jansen, G.H., Rensen, M.G., Schrama, L.H., van Veelen, C.W., van Rijen, P.C., van Nieuwenhuizen, O., Gispen, W.H., de Graan, P.N.,

2002. Distribution of glutamate transporters in the hippocampus of patients with pharmaco-resistant temporal lobe epilepsy. Brain 125, 32–43.
Racine, R.J., 1972. Modification of seizure activity by electrical stimulation. II. Motor seizure. Electroencephalogr. Clin. Neurophysiol. 32, 281–294.
Raju, K., Doulias, P.T., Evans, P., Krizman, E.N., Jackson, J.G., Horyn, O., Daikhin, Y., Nissim, I., Yudkoff, M., Sharp, K.A., Robinson, M.B., Ischiropoulos, H., 2015. Regulation of Brain Glutamate Metabolism by Nitric Oxide and S-nitrosylation. Sci Signal 8, ra68.
Ransom, B., Behar, T., Nedergaard, M., 2003. New roles for astrocytes (stars at last). Trends Neurosci. 26, 520–522.
Ransom, B.R., Ransom, C.B., 2012. Astrocytes: multitalented stars of the central nervous system. Methods Mol. Biol. 814, 3–7.
Rash, J.E., Yasumura, T., Hudson, C.S., Agre, P., Nielsen, S., 1998. Direct immunogold labeling of aquaporin-4 in square arrays of astrocyte and ependymocyte plasma membranes in rat brain and spinal cord. Proc. Natl. Acad. Sci. U. S. A. 95, 11981–11986.
Riban, V., Bouilleret, V., Pham-Le, B.T., Fritschy, J.M., Marescaux, C., Depaulis, A., 2002. Evolution of hippocampal epileptic activity during the development of hippocampal sclerosis in a mouse model of temporal lobe epilepsy. Neuroscience 112, 101–111.
Robel, S., Buckingham, S.C., Boni, J.L., Campbell, S.L., Danbolt, N.C., Riedemann, T., Sutor, B., Sontheimer, H., 2015. Reactive astrogliosis causes the development of spontaneous seizures. J. Neurosci. 35, 3330–3345.
Rothstein, J.D., Dykes-Hoberg, M., Pardo, C.A., Bristol, L.A., Jin, L., Kuncl, R.W., Kanai, Y., Hediger, M.A., Wang, Y., Schielke, J.P., Welty, D.F., 1996. Knockout of glutamate transporters reveals a major role for astroglial transport in excitotoxicity and clearance of glutamate. Neuron 16, 675–686.
Rothstein, J.D., Martin, L., Levey, A.I., Dykes-Hoberg, M., Jin, L., Wu, D., Nash, N., Kuncl, R.W., 1994. Localization of neuronal and glial glutamate transporters. Neuron 13, 713–725.
Sakurai, M., Kurokawa, H., Shimada, A., Nakamura, K., Miyata, H., Morita, T., 2015. Excitatory amino acid transporter 2 downregulation correlates with thalamic neuronal death following kainic acid-induced status epilepticus in rat. Neuropathology 35, 1–9.
Samuelsson, C., Kumlien, E., Flink, R., Lindholm, D., Ronne-Engstrom, E., 2000. Decreased cortical levels of astrocytic glutamate transport protein GLT-1 in a rat model of posttraumatic epilepsy. Neurosci. Lett. 289 (3), 185–188.
Simantov, R., Crispino, M., Hoe, W., Broutman, G., Tocco, G., Rothstein, J.D., Baudry, M., 1999. Changes in expression of neuronal and glial glutamate transporters in rat hippocampus following kainate-induced seizure activity. Brain Res. Mol. Brain Res. 65 (1), 1112–1123.
Skucas, V.A., Mathews, I.B., Yang, J., Cheng, Q., Treister, A., Duffy, A.M., Verkman, A.S., Hempstead, B.L., Wood, M.A., Binder, D.K., Scharfman, H.E., 2011. Impairment of select forms of spatial memory and neurotrophin-dependent synaptic plasticity by deletion of glial aquaporin-4. J. Neurosci. 31, 6392–6397.
Stringer, J.L., 1996. Repeated seizures increase GFAP and vimentin in the hippocampus. Brain Res. 717, 147–153.
Strohschein, S., Hüttmann, K., Gabriel, S., Binder, D.K., Heinemann, U., Steinhäuser, C., 2011. Impact of aquaporin-4 channels on K+ buffering and gap junction coupling in the hippocampus. Glia 59, 973–980.
Szu, J.I., Binder, D.K., 2016. The role of astrocytic aquaporin-4 in synaptic plasticity and learning and memory. Front. Integr. Neurosci. 10, 8.
Tanaka, K., Watase, K., Manabe, T., Yamada, K., Watanabe, M., Takahashi, K., Iwama, H., Nishikawa, T., Ichihara, N., Kikuchi, T., Okuyama, S., Kawashima, N., Hori, S., Takimoto, M., Wada, K., 1997. Epilepsy and exacerbation of brain injury in mice lacking the glutamate transporter GLT-1. Science 276, 1699–1702.
Tessler, S., Danbolt, N.C., Faull, R.L., Storm-Mathisen, J., Emson, P.C., 1999. Expression of the glutamate transporters in human temporal lobe epilepsy. Neuroscience 88, 1083–1091.
Torre, E.R., Lothman, E., Steward, O., 1993. Glial response to neuronal activity: GFAP-mRNA and protein levels are transiently increased in the hippocampus after seizures. Brain Res. 631, 256–264.
Ueda, Y., Doi, T., Tokumaru, J., Yokoyama, H., Nakajima, A., Mitsuyama, Y., Ohya-Nishiguchi, H., Kamada, H., Willmore, L.J., 2001. Collapse of extracellular glutamate regulation during epileptogenesis: down-regulation and functional failure of glutamate transporter function in rats with chronic seizures induced by kainic acid. J. Neurochem. 76 (3), 892–900.
van der Hel, W.S., Notenboom, R.G., Bos, I.W., van Rijen, P.C., van Veelen, C.W., de Graan, P.N., 2005. Reduced glutamine synthetase in hippocampal areas with neuron loss in temporal lobe epilepsy. Neurology 64, 326–333.
Verkman, A.S., 2005. More than just water channels: unexpected cellular roles of aquaporins. J. Cell Sci. 118, 3225–3232.
Volterra, A., Meldolesi, J., 2005. Astrocytes, from brain glue to communication elements: the revolution continues. Nat. Rev. Neurosci. 6, 626–640.
Wetherington, J., Serrano, G., Dingledine, R., 2008. Astrocytes in the epileptic brain. Neuron 58, 168–178.
Yang, J., Li, M.X., Luo, Y., Chen, T., Liu, J., Fang, P., Jiang, B., Hu, Z.L., Jin, Y., Chen, J.G., Wang, F., 2013. Chronic ceftriaxone treatment rescues hippocampal memory deficit in AQP4 knockout mice via activation of GLT-1. Neuropharmacology 75, 213–222.
Yang, L., Li, F., Zhang, H., Ge, W., Mi, C., Sun, R., Liu, C., 2009. Astrocyte activation and memory impairment in the repetitive febrile seizures model. Epilepsy Res. 86, 209–220.